Molecular Therapy
Oncolytics
Original Article

Overcoming resistance of stroma-rich pancreatic cancer with focal adhesion kinase inhibitor combined with G47Δ and immune checkpoint inhibitors

Tomoharu Yamada,[1,2] Ryosuke Tateishi,[2] Miwako Iwai,[1] Minoru Tanaka,[1] Hideaki Ijichi,[2] Makoto Sano,[2] Kazuhiko Koike,[2] and Tomoki Todo[1]

[1]Division of Innovative Cancer Therapy, Advanced Clinical Research Center, and Department of Surgical Neuro-Oncology, The Institute of Medical Science, The University of Tokyo, 4-6-1 Shirokanedai, Minato-ku, Tokyo 108-8639, Japan; [2]Department of Gastroenterology, Graduate School of Medicine, The University of Tokyo, 7-3-1 Hongo, Bunkyo-ku, Tokyo 113-8655, Japan

Pancreatic ductal adenocarcinoma (PDAC) is a lethal disease known for its dense tumor stroma. Focal adhesion kinase inhibitor (FAKi), a non-receptor type tyrosine kinase inhibitor, reduces the tumor stroma. G47Δ, a third-generation oncolytic herpes simplex virus type 1, destroys tumor cells selectively and induces antitumor immune responses. This study evaluates the efficacy of FAKi and G47Δ in PDAC models in combination with or without immune checkpoint inhibitors. G47Δ was effective in human PDAC cell lines *in vitro* and in subcutaneous as well as orthotopic tumor models. Transgenic mouse-derived #146 cells were used to generate subcutaneous PDAC tumors with rich stroma in immunocompetent mice. In this #146 tumor model, the efficacy of FAKi was synergistically augmented when combined with G47Δ, which reflected not only a decreased stromal content but also a significant shifting of the tumor microenvironment toward immune stimulation. In transgenic autochthonous PKF mice, a rare model that develops stroma-rich PDAC with a 100% penetrance and resembles human PDAC in various aspects, the prolongation of survival compared with FAKi alone was achieved only when FAKi was combined with G47Δ and immune checkpoint inhibitors. The FAKi combination therapy may be useful to overcome the treatment resistance of stroma-rich PDAC.

INTRODUCTION

Pancreatic ductal adenocarcinoma (PDAC) is one of the most aggressive cancers and expected to be the second leading cause of cancer-related deaths in the United States by 2030.[1] Only a few chemotherapies are available to date, with limited efficacy.[2]

Oncolytic viruses can selectively replicate in and destroy cancer cells. Herpes simplex virus type 1 (HSV-1) is suited for cancer therapy because it can infect a wide variety of cancer cells with strong cytotoxicity and induce specific antitumor immune responses, without damaging the normal tissues. G47Δ (teserpaturev) is a triple-mutated, third-generation oncolytic HSV-1, noted for its markedly enhanced antitumor activity *in vivo*.[3] G47Δ is found effective for a variety of cancers,[4-10] and it has been tested in patients with glioblastoma,[11] prostate cancer, olfactory neuroblastoma, and malignant mesothelioma. Based on the results of the phase II study, G47Δ was recently approved as a new drug for malignant glioma in Japan.[12] Talimogene laherparepvec (T-VEC), a double-mutated oncolytic HSV-1 expressing granulocyte-macrophage colony-stimulating factor (GM-CSF), showed significant durable responses in patients with advanced melanoma, and it was approved as the first oncolytic virus product in the United States and Europe in 2015.[13] Oncolytic poliovirus reportedly caused a long-term survival in some patients with glioblastoma in a phase I clinical trial.[14] The use of oncolytic viruses for human PDAC has so far been quite limited: HF10, a naturally attenuated HSV-1, was injected intraoperatively into non-resectable pancreatic cancer in six patients, and though safe, only one patient showed a partial response.[15] ONYX-015, an E1B-55 kDa gene-deleted adenovirus, has been tested in clinical trials, but it has not advanced beyond phase I/II.[16,17]

A dense tumor stroma has always been a hurdle for treating PDAC. Focal adhesion kinase inhibitor (FAKi) is a non-receptor type tyrosine kinase inhibitor that can reduce the tumor stroma, recruit cytotoxic T lymphocytes (CTLs), and suppress regulatory T cells (Tregs) in the tumor microenvironment by regulating transcription of chemokines.[18,19] Whether FAKi can improve the efficacy of immune checkpoint inhibitors (ICIs) in solid malignancies is a topic currently under investigation.

Received 27 May 2022; accepted 5 December 2022;
https://doi.org/10.1016/j.omto.2022.12.001.

Correspondence: Tomoki Todo, M.D., Ph.D., Division of Innovative Cancer Therapy, Advanced Clinical Research Center, and Department of Surgical Neuro-Oncology, The Institute of Medical Science, The University of Tokyo, Tokyo 108-8639, Japan.
E-mail: toudou-nsu@umin.ac.jp

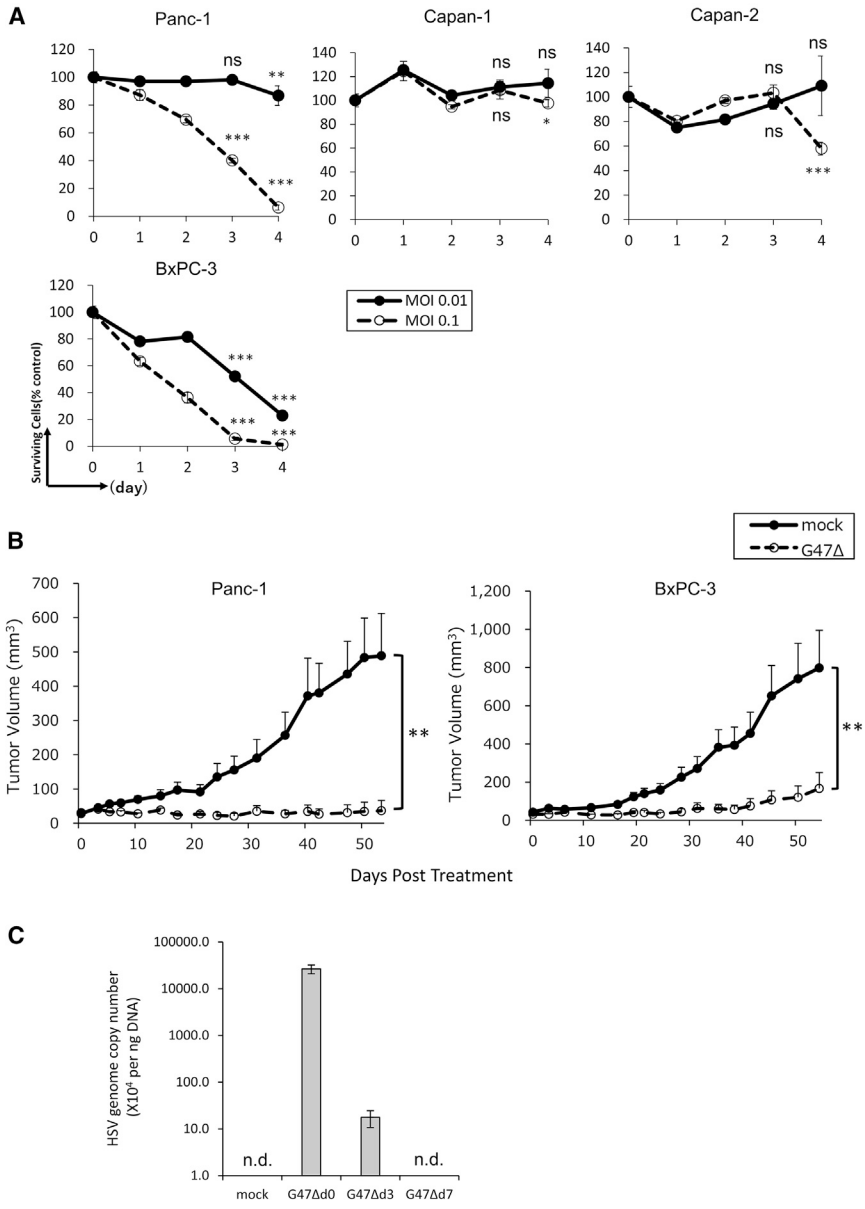

Figure 1. The antitumor effect of G47Δ in human PDAC cells *in vitro* and *in vivo*

(A) Cytopathic effect of G47Δ *in vitro*. The number of surviving cells of Panc-1, Capan-1, Capan-2, and BxPC-3 cells after infection with G47Δ at an MOI of 0.01 or 0.1 is counted on indicated days and expressed as percentage of number of mock-infected control cells. The results are shown as the means (n = 3); error bars indicate SD. (B) Efficacy of G47Δ in athymic mice bearing subcutaneous Panc-1 or BxPC-3 tumors. In both subcutaneous tumor models, intratumoral inoculations with G47Δ (2×10^6 pfu) on days 0 and 3 caused a significant inhibition of tumor growth. The results are presented as mean (n = 7); error bars represent SEM. Tumor volume = length × width × height/2. (C) Replication of G47Δ in the normal pancreas. The normal pancreases of A/J mice were injected with G47Δ (1×10^7 pfu) and removed on days 0, 3, and 7 or with mock and removed on day 0. A high number of G47Δ copies was detected by qPCR from the pancreas on day 0, but the number rapidly decreased on day 3, reflecting no replication of G47Δ in the normal pancreas. The results are presented as mean (n = 3); error bars represent SEM. *p < 0.05, **p < 0.01, ***p < 0.001; vs. mock-infected controls. ns; not significant. n.d.; not detected.

Immunotherapy has changed the treatment strategies of cancer, especially for malignant melanoma, lung cancer, kidney cancer, and head and neck cancer.[20] None of the ICIs, however, has shown efficacy in treating PDAC.[21-24] In order to induce therapeutic effects of ICIs, various combination therapies are under investigation, including chemotherapy, radiotherapy, vaccines, and oncolytic viruses. Several clinical studies combining chemotherapy, such as gemcitabine, with ICIs have failed in improving the outcome.[24] For ICIs to work in PDAC, it would be necessary to use therapeutic means that can recruit CTLs and turn an immunologically "cold" PDAC into a "hot" tumor. In this regard, G47Δ with FAKi and ICIs may serve as an optimal combination in treating PDAC.[25]

In this study, we show that the combination of G47Δ with FAKi exhibits synergistic therapeutic effect on PDAC. Further, using PKF mice, a transgenic autochthonous mouse model that reproduces the natural course of PDAC in human, we demonstrate that a combination of G47Δ and FAKi, with anti-PD-L1 and anti-CTLA4 antibodies, results in enhanced efficacy.

RESULTS

G47Δ shows oncolytic activity in human PDAC cells

Four human PDAC cell lines (Panc-1, Capan-1, Capan-2, and BxPC-3) were used to evaluate the cytopathic effects of G47Δ *in vitro*. Cells were infected with G47Δ at a multiplicity of infection (MOI) of 0.1 or 0.01. In Panc-1 and BxPC-3 cells, G47Δ showed significant cytopathic effect, eradicating more than 90% of tumor cells on post-infection day 4 at an MOI of 0.1. However, G47Δ showed limited effect in Capan-1 and Capan-2 cells (Figure 1A).

The infectivity of G47Δ was evaluated by X-gal staining using Vero cells as control. At an MOI of 3, Panc-1, Capan-2, and BxPC-3 cells showed efficient infection with G47Δ, although Capan-1 demonstrated limited infectivity (Figure S1A). Further, we evaluated the replication capability of G47Δ by virus replication assay. G47Δ replicates efficiently in Panc-1 and BxPC-3 cells and to a certain extent in Capan-2 cells, but not in Capan-1 cells (Figure S1B).

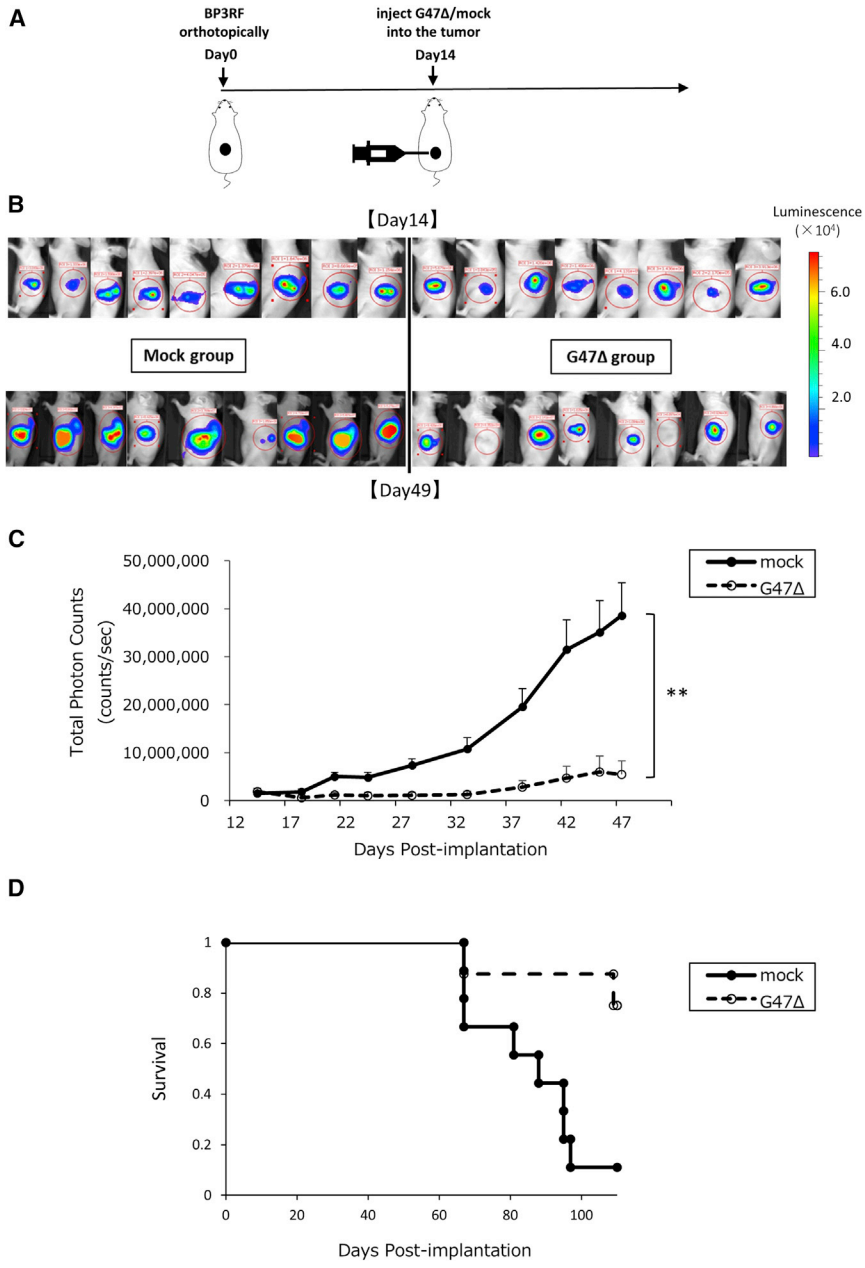

Figure 2. The efficacy of G47Δ in an orthotopic human pancreatic cancer model

(A) The experimental schedule. Orthotopic PDAC is generated in the pancreas of athymic mice using BxPC-3-Red-Fluc cells (1×10^6) and treated with a single intratumoral injection with G47Δ (2×10^6 pfu) (n = 8) or mock (n = 9) on day 14. (B) The tumor growth was evaluated by measuring the total photon counts by IVIS. (C) G47Δ treatment significantly inhibited the growth of orthotopic PDAC in athymic mice ($p < 0.01$). The data are the means; error bars indicate SEM. **$p < 0.01$. (D) Kaplan-Meier analysis reveals that G47Δ treatment significantly prolongs the survival of athymic mice with orthotopic PDAC ($p < 0.01$, log rank test).

G47Δ is effective against human PDAC tumors *in vivo*

Subcutaneous tumors of Panc-1 and BxPC-3 cells were generated in athymic mice (n = 7), and G47Δ (2×10^6 plaque-forming units [pfu]) was intratumorally administered on days 0 and 3. G47Δ caused a significant inhibition of the tumor growth in both subcutaneous tumor models (Figure 1B).

To simulate the clinical settings, orthotopic PDAC was generated in the pancreas of athymic mice using BxPC-3-Red-Fluc cells, and established tumors were treated with a single intratumoral injection with G47Δ (2×10^6 pfu) on day 14 (Figure 2A). The tumor growth was then followed by measuring the total flux by In Vivo Imaging System (IVIS). Treatment with G47Δ significantly inhibited the tumor growth compared with mock ($p < 0.01$ at day 49; Figures 2B and 2C). Six of eight mice survived in the G47Δ group, whereas only one of nine mice survived in the mock group ($p < 0.01$; Figure 2D). Thus, intratumoral injections with G47Δ in the pancreas are shown useful for treating PDAC in these models.

Replication and cytotoxicity of G47Δ in the normal pancreas

To evaluate the replication and cytotoxicity of G47Δ in the normal pancreas, the normal pancreases of HSV-1-sensitive A/J mice were injected with G47Δ (1×10^7 pfu) or mock and removed on days 0, 3, and 7. A high number of G47Δ copies was detected by qPCR from the pancreas as expected on day 0 ($2.6 \times 10^8 \pm 5.7 \times 10^7$/ng DNA [mean ± SEM]), the number rapidly decreased by day 3 to the detection limit level ($1.8 \times 10^5 \pm 0.4 \times 10^5$/ng DNA), and G47Δ was no longer detected on day 7 (Figure 1C). The result indicates that G47Δ does not replicate in the normal pancreas. Histopathology of the pancreases stained with H&E or immunostained with an anti-HSV-1 antibody revealed no abnormalities at any time point after injection for both G47Δ and mock (Figure S2), implicating that G47Δ causes no cytotoxicity in the normal pancreas.

G47Δ and FAKi act synergistically for tumor growth inhibition of PDAC

As PDAC is associated with rich stroma, we used FAKi that acts to reduce the tumor stroma. A murine PDAC cell line, #146, derived from *Pdx1*$^{cre/+}$;*LSL-Kras*$^{G12D/+}$;*Trp53*$^{fl/+}$ mice, was infected in culture with G47Δ at an MOI of 1 or 3 and treated with 0.005, 0.05, or 0.5 μM of FAKi. G47Δ showed significant cytopathic effects by day 3 at both

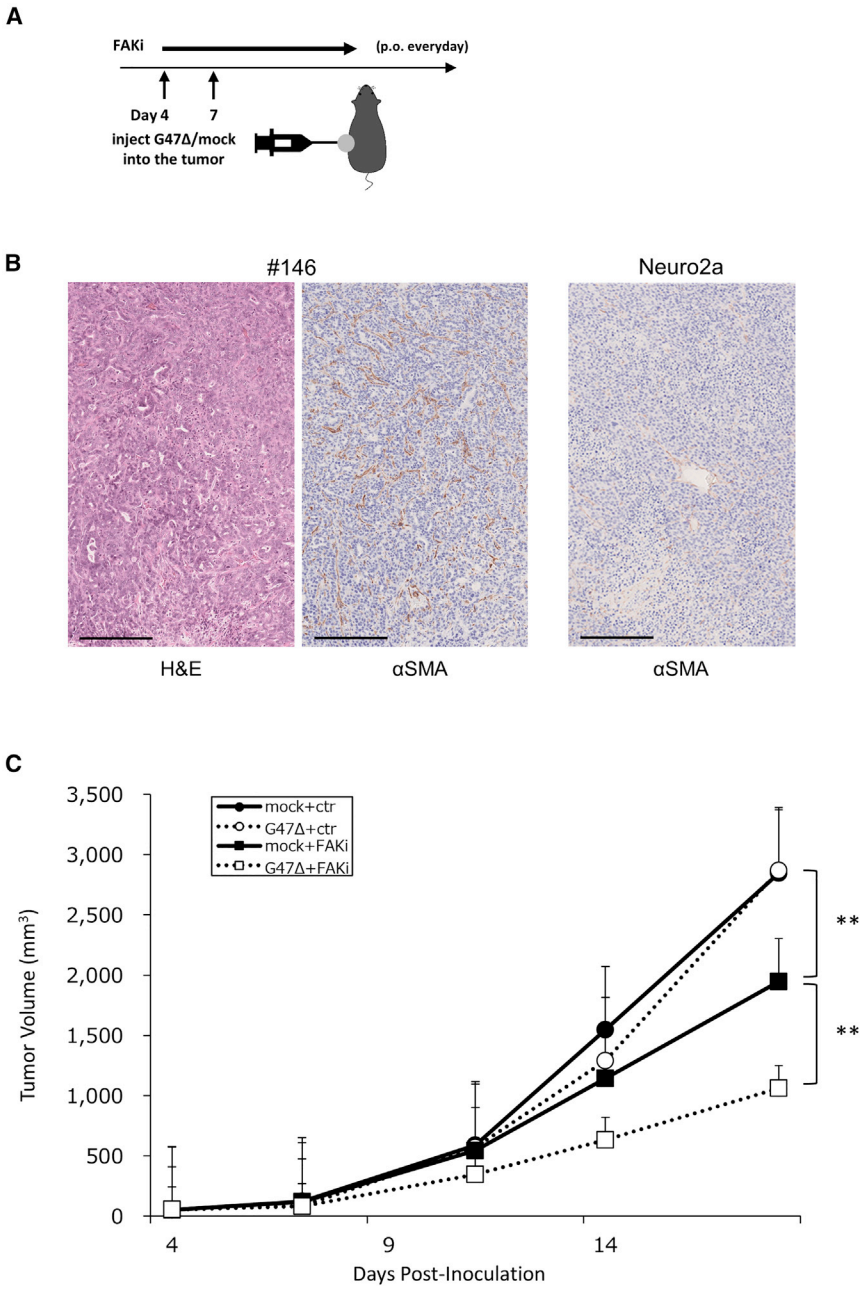

Figure 3. G47Δ combined with FAKi synergistically inhibits tumor growth

(A) The experimental schedule. C57BL/6NCrSlc male mice with established subcutaneous #146 tumors were treated with intratumoral injections with G47Δ (2×10^6 pfu) or mock on days 4 and 7, without or with daily oral administrations with FAKi (50 mg/kg) from day 4. (B) Representative histology images of subcutaneous #146 tumor stained with H&E and immunostained with an anti-αSMA antibody showing rich stroma. A histology image of subcutaneous Neuro2a tumor with αSMA immunostaining representing a tumor with poor stroma is presented for comparison. (C) G47Δ and FAKi acted synergistically, and the combination led to a greater inhibition of the tumor growth than the FAKi monotherapy. The data are the means (n = 7); error bars represent SEM. Tumor volume = length × width × height/2. **$p < 0.01$. Scale bar, 200 μm.

MOI of 1 and 3 and positive infection of #146 cells (Figures S3A and S3D). Treatment with FAKi alone at 0.05 μM and 0.5 μM killed more than 90% of the cells by day 4 (Figure S3B). Whereas FAKi alone at a low concentration of 0.005 μM showed no cytotoxic effect on day 3, it significantly augmented the cytopathic effect of G47Δ at an MOI of 1 when combined ($p = 0.002$ and $p < 0.001$ for day 3 and day 4, respectively, G47Δ vs. FAKi+G47Δ; Figure S3C).

We then generated subcutaneous tumors of #146 cells in the flanks of C57BL/6NCrSlc mice. The histology of established tumors showed rich stroma, mimicking human PDAC (Figures 3A and 3B). Animals were treated with intratumoral injections with G47Δ (2×10^6 pfu) or mock on days 4 and 7, with or without daily oral administrations with FAKi (50 mg/kg) from day 4. Whereas the treatment with G47Δ alone showed no antitumor efficacy, that with FAKi alone inhibited the tumor growth compared with control ($p < 0.01$ on day 18; Figure 3C). Consistent with *in vitro* studies, the combination of G47Δ and FAKi led to a significantly greater inhibition of the tumor growth than the FAKi monotherapy ($p < 0.01$ on day 18; Figure 3C). The expected and observed fractional tumor volumes (FTVs) with this combined treatment on day 18 were 0.690 and 0.373, respectively. Since the expected FTV to observed FTV ratio was >1 (1.85), G47Δ and FAKi were considered to have a synergistic effect.

The combination therapy modifies tumor microenvironment toward immune stimulation

To investigate the immunological aspect of how tumor microenvironment is altered by the combination therapy using G47Δ and FAKi, single cells prepared from treated tumors, including tumor infiltrating lymphocytes (TILs), were evaluated by flow cytometric analysis (Figure 4A). The numbers of $CD8^+$ and $CD4^+$ T cells, natural killer (NK) cells, Tregs, tumor-associated macrophages (TAMs), CD69- or CD25-positive $CD8^+$ and $CD4^+$ T cells and myeloid-derived suppressive cells (MDSCs), and the PD-L1 expression status were evaluated. Flow cytometry gating strategy for an individual cell subset is shown in Figure S4A.

The combination therapy caused a significant increase of the proportions of both $CD8^+$ T cells and $CD4^+$ T cells among $CD45^+$ cells

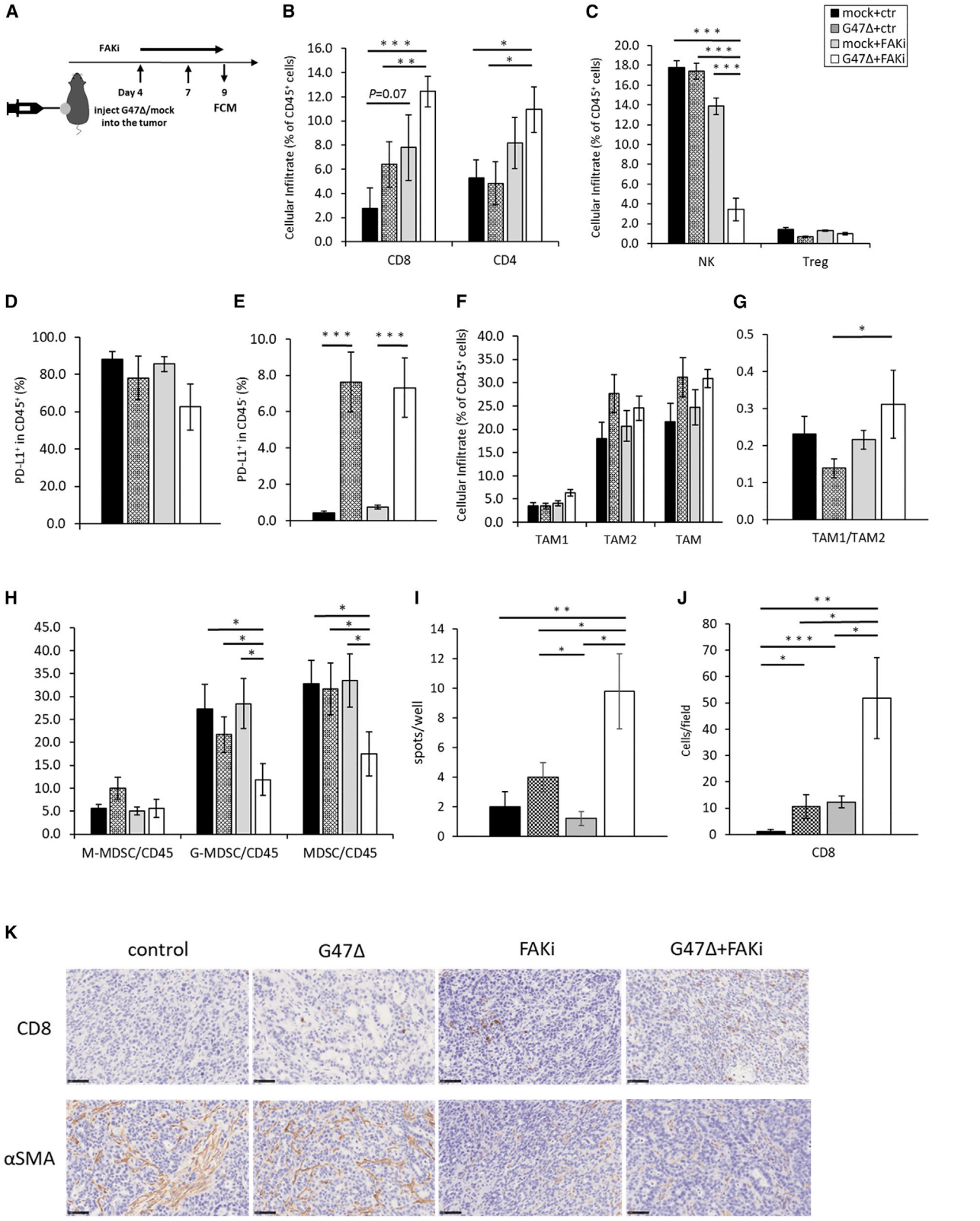

(legend on next page)

compared with control or G47Δ monotherapy ($p < 0.001$ and $p < 0.05$, respectively vs. control; $p < 0.01$ and $p < 0.05$, respectively vs. G47Δ alone: Figure 4B). The combination therapy as well as G47Δ alone significantly increased the proportions of $CD8^+CD69^+$ T cells ($p < 0.001$ for both G47Δ and G47Δ+FAKi) and $CD8^+CD25^+$ T cells ($p < 0.01$ for both G47Δ and G47Δ+FAKi; Figure S4B), whereas such was not observed with $CD4^+$ T cells (Figure S4C). In contrast, the proportion of NK cells among $CD45^+$ cells was significantly decreased by the combination therapy compared with all other treatments ($p < 0.001$ vs. each treatment; Figure 4C). Tregs and PD-$L1^+CD45^+$ cells were both neither affected by G47Δ nor FAKi (Figures 4C and 4D). Treatment with G47Δ caused a significant increase of the proportion of PD-$L1^+$ cells among $CD45^-$ tumor cells with or without FAKi, whereas FAKi alone had no effect on the PD-L1 expression of tumor cells (G47Δ vs. control, $p < 0.001$; G47Δ + FAKi vs. FAKi, $p < 0.001$; Figure 4E). The TAM1/TAM2 ratio did not change by treatment with G47Δ alone, but significantly increased when combined with FAKi (G47Δ vs. G47Δ + FAKi, $p < 0.05$; Figures 4F and 4G). The combination therapy caused a significant decrease of the MDSC proportion compared with all other treatments, reflecting the decease of the granulocytic-MDSC (G-MDSC) proportion ($p < 0.05$ vs. each treatment: Figure 4H).

To assess tumor-specific immune responses induced by the combination of G47Δ and FAKi, ELISpot assay was performed using splenocytes harvested from subcutaneous #146 tumor-bearing mice on day 9 of treatment. The combination therapy caused a significant increase in the number of #146 cell-reactive splenocytes compared with other therapies ($p < 0.01$, $p < 0.05$, and $p < 0.05$ vs. control, G47Δ alone, and FAKi alone, respectively; Figure 4I).

Subcutaneous #146 tumors of treated animals were further assessed by immunohistochemistry. The combination therapy caused a significant increase in the number of infiltrating $CD8^+$ T cells compared with other treatments ($p < 0.01$, $p < 0.05$, and $p < 0.05$ vs. mock, G47Δ, and FAKi, respectively; Figures 4J and 4K). Immunostainings for αSMA revealed that treatment with FAKi caused a remarkable decrease of stroma (Figure 4K). Quantitative polymerase chain reaction (qPCR) analysis for G47Δ revealed that combining FAKi had no effect on *in vivo* replication of G47Δ in subcutaneous #146 tumors (Figure S5). The levels of serum cytokines, including IFN-γ, IL-2, IL-4, IL-5, IL-6, IL-10, IL-12, TNFα, and GM-CSF were measured 1, 4, and 11 days after the second administration with G47Δ. No significant difference was observed in any of the cytokines among four treatment groups (Figure S6). The results indicate that the combination therapy modifies the tumor microenvironment toward immune stimulation.

G47Δ with or without ICIs is inefficacious in transgenic PKF mice

Next, to explore whether G47Δ is efficacious for a naturally occurring, stroma-rich PDAC, we used PKF (*Ptf1a*$^{cre/+}$;*LSL-Kras*$^{G12D/+}$;*Tgfbr2*$^{fl/fl}$) autochthonous PDAC mice. This transgenic mouse model mimics human PDAC on various aspects.[26,27] PKF mice develop well-differentiated PDAC with a 100% penetrance, and they all die of a tumor burden with a median survival of 59 days. They manifest weight loss, bloody ascites, and jaundice, resembling a common clinical course of human PDAC. Tumors appear from 5 weeks old with no exception and eventually occupy the entire pancreas. Histology shows well-differentiated glandular architecture with rich stromal component, again mimicking human PDAC.

42-day-old PKF mice were randomly divided into four treatment groups (n = 6 per group). Mice were treated with a single intratumoral injection with G47Δ (1×10^7 pfu) or mock, with or without intraperitoneal injections with anti-PD-L1 (200 μg/body) and anti-CTLA4 (250 μg/body) antibodies every 4–5 days (Figure 5A). Kaplan-Meier analysis revealed no difference in survival among four treatment groups (log rank test; Figure 5B). Typical pancreatic tumors of 46-day-old PKF mice show rich stroma (Figure 5C). When G47Δ (1×10^7 pfu) is injected into a pancreatic tumor of a PKF mouse, immunostaining with an anti-HSV-1 antibody demonstrates positivity for HSV-1 on day1 but not on day 3 of G47Δ injection (Figure 5D). *In vivo* replication study in subcutaneous tumors generated with K399, a murine PDAC cell line derived from PKF mice, showed a relatively high number of G47Δ copies recovered until 2 days after intratumoral G47Δ injection, but G47Δ copies decreased rapidly by day 3, implicating that G47Δ replication capability in PKF tumor model is limited (Figure 5E).

The efficacy of FAKi is augmented when combined with G47Δ and immune checkpoint inhibitors in transgenic PKF mice

Because the combination of FAKi with G47Δ shifted tumor microenvironment toward immune stimulation and decreased areas of stroma in #146 tumors, we further investigated whether an additional combination of FAKi causes a favorable effect in PKF mice. It has been reported that FAKi alone can prolong the survival of KPC mice, another transgenic PDAC mouse model.[18] 42-day-old PKF mice were randomly divided into four treatment groups (n = 10, mock and FAKi groups; n = 9, FAKi + G47Δ and FAKi + G47Δ + ICIs groups). In addition to an intratumoral injection with G47Δ (1×10^7 pfu), or

Figure 4. The combination therapy modifies tumor microenvironment toward immune stimulation

(A) The experimental schedule. C57BL/6NCrSlc male mice with established subcutaneous #146 tumors were treated with intratumoral injections with G47Δ (2×10^6 pfu) or mock on days 4 and 7, without or with daily oral administrations with FAKi (50 mg/kg) from day 4. Tumors were collected on day 9 and single cells prepared. Results of flow cytometric analyses are shown for (B) $CD8^+$ lymphocytes and $CD4^+$ lymphocytes; (C) NK cells and Treg; (D) $CD45^+$PD-$L1^+$ cells; (E) PD-$L1^+$ tumor cells; (F) TAM1,TAM2 and TAM (TAM1 + TAM2) cells; (G) TAM1/TAM2 ratio; and (H) M-MDSC and G-MDSC. The data are the means (n = 5); error bars represent SEM. (I) ELISpot assay. Splenocytes were collected on day 9 and subjected to ELISpot assay for IFN-γ secretion in response to stimulation by #146 cells. The data are the means (n = 3); error bars represent SEM. (J) The numbers of $CD8^+$ cells in subcutaneous #146 tumors. $CD8^+$ cells were counted in five fields per section. The data are the means (n = 3); error bars represent SEM. (K) Representative immunohistochemical images of subcutaneous #146 tumors immunostained with anti-CD8 and anti-αSMA antibodies. *$p < 0.05$, **$p < 0.01$, ***$p < 0.001$. Scale bar, 100 μm.

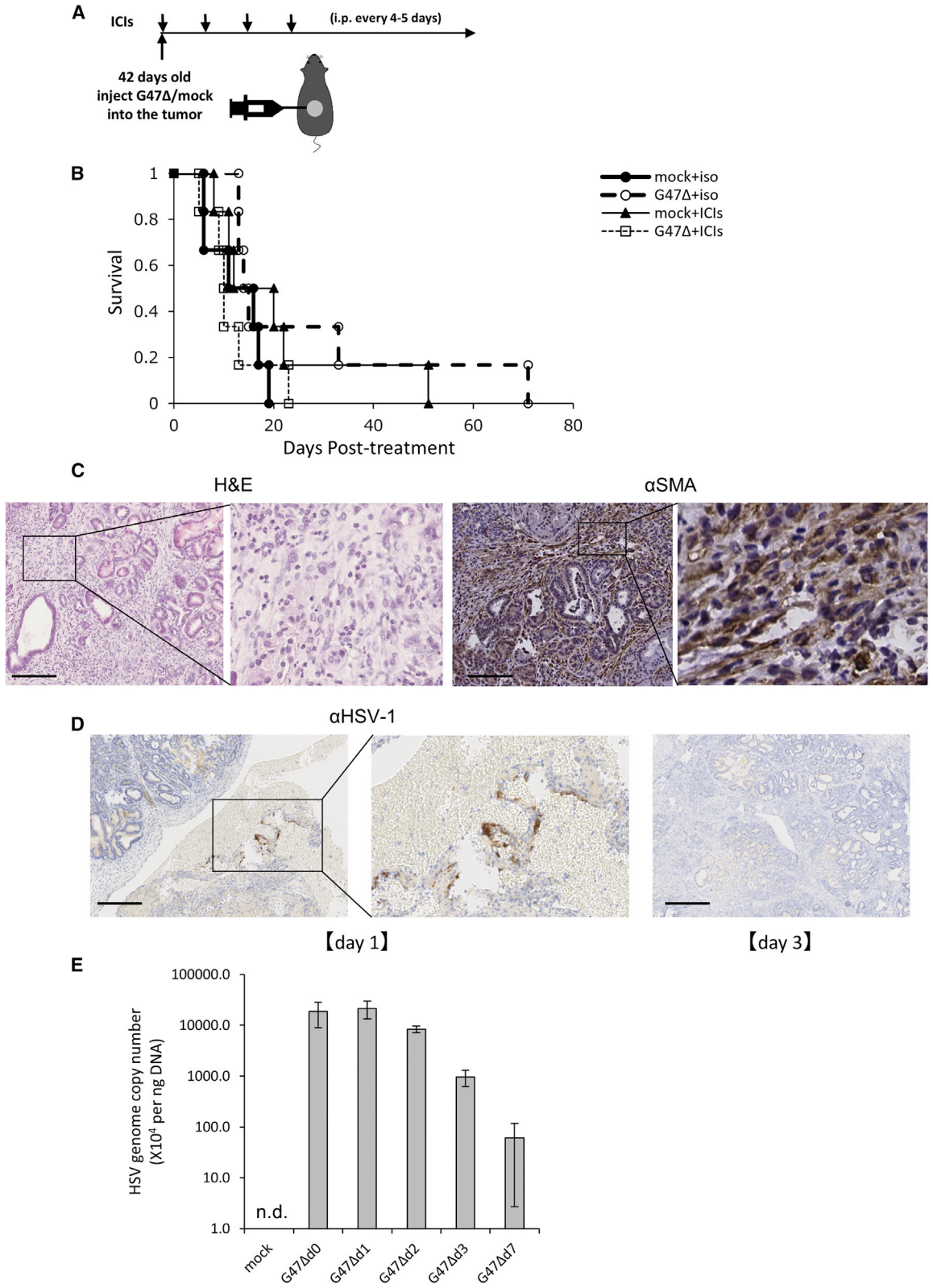

(legend on next page)

G47Δ treatment combined with intraperitoneal injections with anti-PD-L1 (200 μg/body) and anti-CTLA4 (250 μg/body) antibodies every 4–5 days, mice were treated with oral administration with FAKi (50 mg/kg) daily (Figure 6A). Control groups received an intratumoral injection with mock with or without daily FAKi administration. Treatment with FAKi alone prolonged the survival of PKF mice compared with control ($p = 0.0001$). Contrarily to our expectation, FAKi combined with G47Δ treatment showed no enhancing effect over FAKi alone. However, combining FAKi treatment with G47Δ and ICIs led to a significant improvement of survival compared with FAKi alone ($p = 0.0087$) or FAKi + G47Δ ($p = 0.0091$; Figure 6B). Immunohistochemical analysis of pancreatic tumors of PKF mice for αSMA demonstrated that all treatments that included FAKi significantly decreased the tumor stroma compared with control (Figure 6C). The triple combination treatment, FAKi + G47Δ + ICIs, caused a remarkable increase of the infiltration of both $CD4^+$ and $CD8^+$ T cells, but not NK cells (Figure 6C). $TAM1^+$ and $TAM2^+$ cells were prominent in all groups without apparent differences (Figure 6C).

Prior to the above experiment, we performed an experiment comparing the efficacy of FAKi alone and FAKi + ICIs in PKF mice. The results showed no significant difference in survival between the two treatment groups ($p = 0.387$; Figure S7). Therefore, neither FAKi + G47Δ nor FAKi + ICIs showed increased efficacy over FAKi alone in PKF mice, and the prolongation of survival was achieved only when FAKi was combined with both G47Δ and ICIs.

DISCUSSION

G47Δ, a triple-mutated oncolytic HSV-1, has shown safety and efficacy in several clinical trials.[5,11,12] The phase II trial in glioblastoma patients led to the recent approval of G47Δ as a new drug for malignant glioma in Japan.[12] Here, we show that the treatment resistance of stroma-rich PDAC may be overcome by the use of focal adhesion kinase inhibitor when combined with G47Δ and ICIs.

One of the obstacles in developing new treatments for PDAC has been the lack of proper animal models that reflect the clinical course and histology in human. The transgenic PKF mouse model we use is rare in that it resembles human PDAC in all aspects.[26,27] PKF mice invariably develop PDAC at 5 weeks old and die of tumor burden with a median of 59 days, and the well-differentiated glandular tumor has rich stroma mimicking human PDAC. The significance of the present study is that, because the efficacy of the combination therapy was shown in PKF mice, we can expect such outcome to be reproduced in clinical settings. This model was used to discover that erlotinib showed additional benefit to gemcitabine.[28] We recently demonstrated that anti-VCAM-1 antibody was efficacious in PKF mice.[29] The transgenic KPC mouse (*LSL-Kras$^{G12D/+}$;LSL-Trp53$^{R172H/+}$;Pdx-1-Cre*) has been used as a model for PDAC, but it does not resemble human in that tumors grow rather slowly with the mean survival of 5 months, the tumor stroma is less dense than human, and 8% of KPC mice form sarcoma.[30] Oncolytic vaccinia virus armed with interleukin 10 was shown effective in prolonging the survival of KPC mice.[31]

The dense tumor stroma has always been the main obstacle for treating PDAC. Stroma not only suppresses actions of chemotherapeutic agents, but it contains fibroblasts and extracellular matrix that block infiltration of effector cells.[32] To overcome the stroma problem, several agents have been developed, including the Hedgehog inhibitor (IPI-926) and human hyaluronidase (PEGPH20), but these agents failed to improve the outcome of chemotherapy in PDAC patients.[33,34] FAKi is a promising, non-receptor type tyrosine kinase inhibitor that can act on stroma and inhibit tumor growth of PDAC.[19] It has been reported that various FAK inhibitors, including VS-4718 used in this study, are undergoing clinical trials in different phases.[35] FAKi has shown efficacy in the subcutaneous #146 tumor model presumably by recruiting $CD8^+$ T cells and decreasing Tregs.[18] Whereas G47Δ alone showed efficacy in athymic mice bearing human PDAC tumors, it did not exhibit any effect in immunocompetent mice bearing #146 tumors or in PKF mice. One obvious reason would be that G47Δ does not kill mouse PDAC cells as efficiently as human PDAC cells. It is also possible that G47Δ cannot spread efficiently in a stroma-rich environment. However, FAKi acted synergistically with G47Δ, and the combination was significantly more efficacious than FAKi alone in the subcutaneous #146 tumor model. The combination therapy was shown to modify tumor microenvironment toward immune stimulation, so the synergy is likely a result of immunostimulatory actions of both FAKi and G47Δ. In transgenic autochthonous PKF mice, not only G47Δ alone but also G47Δ with ICIs showed no efficacy: an augmented efficacy was observed only when FAKi was combined with both G47Δ and ICIs. Therefore, the use of FAKi seems required for overcoming the treatment resistance of PDAC. Further, this observation likely shows that, as the mechanism of efficacy augmentation by FAKi, the release of stroma's blockade of immune cell infiltration, thereby augmenting antitumor immune responses, may be acting more importantly than allowance of virus spread. Because G47Δ replicates in and kills human tumor cells more efficiently than mouse tumor cells, a higher efficacy of the combination therapy, using FAKi, G47Δ, and ICIs, may be expected in clinical settings than in the mouse models.

Figure 5. G47Δ with or without ICIs is inefficacious in transgenic PKF mice

(A) The experimental schedule. PKF mice (42 days old) were treated with an intratumoral injection with G47Δ (1×10^7 pfu) or mock, with or without intraperitoneal injections with anti-PD-L1 (200 μg/body) and anti-CTLA4 (250 μg/body) antibodies (n = 6 per group) every 4–5 days. (B) Kaplan-Meier analysis reveals no difference in survival among four treatment groups (log rank test). (C) Representative histology of typical pancreatic tumors of 46-day-old PKF mice using H&E and anti-α SMA staining demonstrates rich stroma. (D) After being injected with G47Δ (1×10^7 pfu), a pancreatic tumor of a PKF mouse shows immuno-positivity for HSV-1 on day 1 but not on day 3. Scale bar, 200 μm. (E) *In vivo* replication study of G47Δ. Subcutaneous K399 tumors in athymic mice were injected with G47Δ (2×10^6 pfu) 7 days after tumor implantation. Tumors were harvested on days 0, 1, 2, 3, and 7 for G47Δ (n = 3–4) and on day 0 for mock (n = 3), and recovered virus was measured by qPCR. Results are the means; error bars represent SEM. n.d.; not detected.

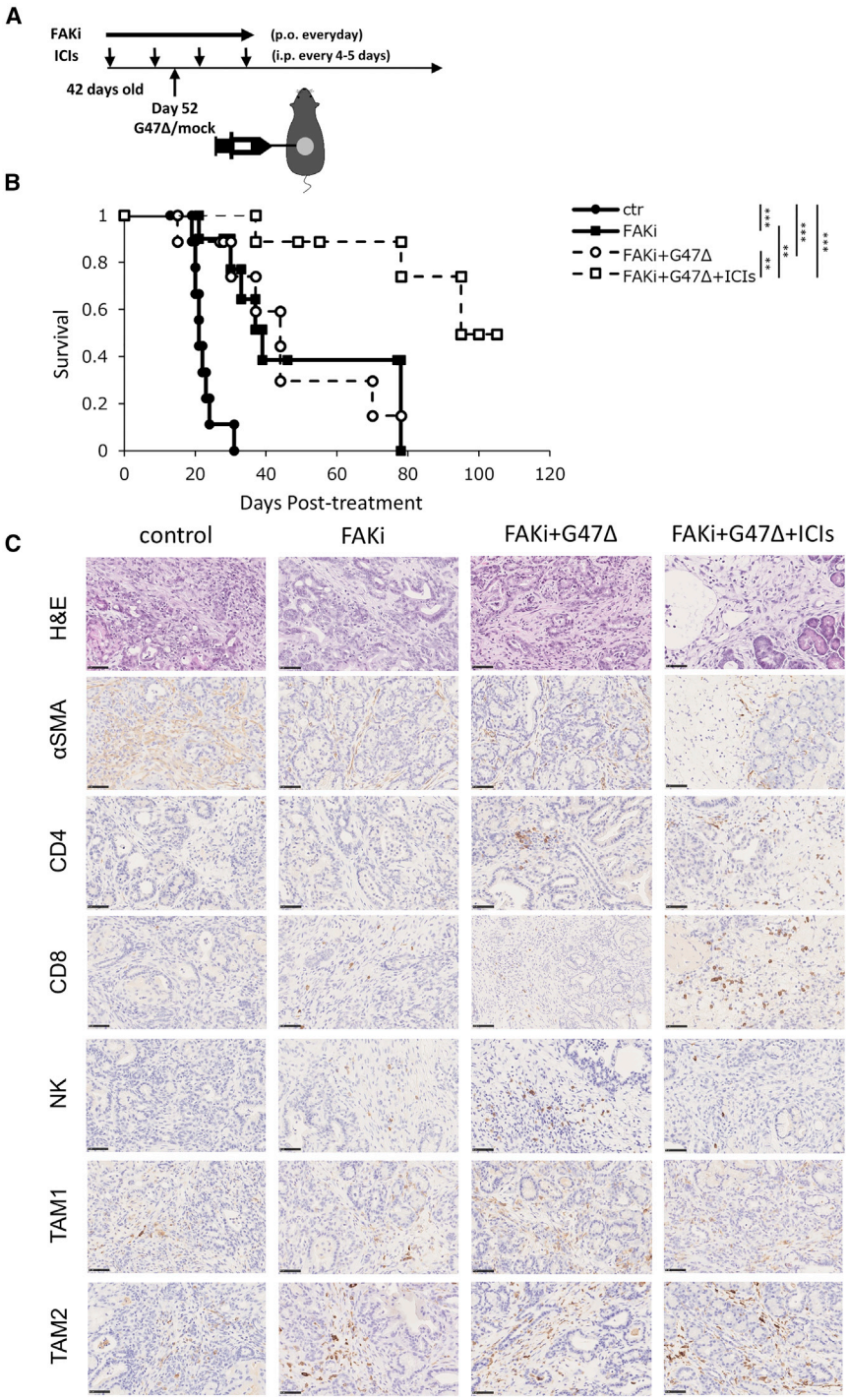

Figure 6. The efficacy of FAKi is augmented when combined with G47Δ and immune checkpoint inhibitors in transgenic PKF mice

(A) The experimental schedule. 42-day-old PKF mice were randomly divided into four treatment groups (n = 10, mock and FAKi groups; n = 9, FAKi + G47Δ and FAKi + G47Δ + ICI groups). In addition to an intratumoral injection with G47Δ (1×10^7 pfu), or G47Δ treatment combined with intraperitoneal injections with anti-PD-L1 (200 μg/body) and anti-CTLA4 (250 μg/body) antibodies every 4–5 days, PKF mice were treated with oral administration with FAKi (50 mg/kg) daily. Control groups received an intratumoral injection with mock with or without daily FAKi administration. (B) Kaplan-Meier analysis demonstrates that the combination of FAKi treatment with G47Δ and ICIs significantly prolongs the survival of PKF mice compared with FAKi alone ($p = 0.0087$) or FAKi + G47Δ ($p = 0.0091$). FAKi alone prolonged the survival of PKF mice compared with control ($p = 0.0001$), but FAKi combined with G47Δ treatment showed no enhancing effect over FAKi alone. *$p < 0.05$, **$p < 0.01$, ***$p < 0.001$. (C) Representative histology of pancreatic tumors of PKF mice in four treatment groups. Sections of pancreatic tumors were stained with H&E, or immunostained for αSMA, CD4, CD8, NK (CD161), TAM1 (CD86) or TAM2 (CD206). Scale bar, 50 μm.

PDAC is known to be an immunologically "cold" tumor, characterized by the presence of dominant immunosuppressive cells such as MDSCs, Tregs, and TAMs in the tumor microenvironment.[36] Our study shows that the combination of FAKi and G47Δ can turn these "cold" tumors "hot." FAKi is reported to inhibit the recruitment of Tregs by decreasing the expression of CCL5,[19] but in the subcutaneous #146 tumor model, we show that the addition of FAKi to G47Δ rather causes enhanced recruitment of $CD8^+$ and $CD4^+$ T cells and a decrease in NK cells, TAM1/TAM2 ratio, and MDSCs in the tumor microenvironment. It has been reported that NK cells and $CD8^+$ T cells exert negative feedback on each other.[37,38] MDSCs are known to suppress the antitumor immunity, and we have reported that an inhibition of CXCR2, expressed on MDSCs, disrupted the tumor-stromal interactions and improved survival in a PDAC mouse model.[39] In addition to the actions of FAKi, G47Δ alone causes a significant increase of $PD\text{-}L1^+$ ratio of tumor cells. Expression levels of PD-L1 are shown to correlate with the effectiveness of immune check point inhibitors.[40]

In conclusion, the efficacy of FAKi was significantly augmented via a synergistic action when combined with G47Δ or with both G47Δ and ICIs in immunocompetent mice bearing stroma-rich PDAC. The combination therapy likely modifies the tumor microenvironment toward immune stimulation. FAKi in combination with G47Δ and ICIs may be useful to overcome the treatment resistance and to improve the outcome of PDAC patients.

MATERIALS AND METHODS

Cell lines and virus

Vero (African green monkey kidney) and human PDAC cell lines, Capan-1, Capan-2, and BxPC-3, were purchased from the American Type Culture Collection (Manassas, VA, USA). The Panc-1 (human PDAC) was purchased from RIKEN Cell Bank (Tsukuba, Japan). BxPC-3-Red-Fluc was purchased from PerkinElmer (Waltham, MA, USA). A murine PDAC cell line, #146, was previously established from the *Pdx1*$^{cre/+}$;*LSL-Kras*$^{G12D/+}$;*Trp53*$^{fl/+}$ mouse model.[41] A murine PDAC cell line, K399, was derived from PKF (*Ptf1a*$^{cre/+}$;*LSL-Kras*$^{G12D/+}$;*Tgfbr2*$^{fl/fl}$) mice.[27] Vero and #146 cells were maintained in DMEM supplemented with 10% fetal bovine serum (FBS). Capan-1 and Capan-2 cells were maintained in IMDM and McCoy's 5A supplemented with 20% and 10% FBS, respectively. The BxPC-3, Panc-1, BxPC-3-Red-Fluc, and K399 cells were maintained in RPMI1640 supplemented with 10% FBS. All the cells were incubated at 37°C under 5% CO_2. G47Δ is a conditionally replicating oncolytic HSV-1 virus with deletions in the *γ34.5* and *α47* genes and an inactivating insertion of the *LacZ* within the *ICP6* locus.[3]

Animal studies

C57BL/6NCrSlc male mice (6 weeks old) and BALB/c *nu/nu* female mice (6–7 weeks old) were purchased from Japan SLC (Hamamatsu, Japan). The PKF (*Ptf1a*$^{cre/+}$;*LSL-Kras*$^{G12D/+}$;*Tgfbr2*$^{fl/fl}$) mice were generated and genotyped as previously described.[26,27] All animal studies were approved by the Ethics Committee for Animal Experimentation of the University of Tokyo.

Subcutaneous tumor models

Subcutaneous tumors were generated by injecting Panc-1 or BxPC-3 cells (5×10^6), or K399 cells (3×10^6) into the left flank of athymic (BALB/c *nu/nu*) mice, and #146 cells (1×10^6) into the left flank of C57BL/6NCrSlc mice. The cells were suspended in 70 μL serum-free medium before injection. In athymic mouse models, when the subcutaneous tumors reached 5 mm in diameter, G47Δ (2×10^6 pfu) or mock (defined as 20 μL PBS supplemented with 10% glycerol) was administered intratumorally on days 0 and 3. Mice were euthanized when tumors reached 24 mm in diameter as regulated by the Ethics Committee for Animal Experimentation of the University of Tokyo. Drug interactions were evaluated as synergistic or additive, using the FTV.[42] The FTV was calculated as the ratio of experimental tumor volume to mean control tumor volume. The expected FTV was calculated as the FTV after FAKi × FTV after G47Δ. If the ratio of the expected FTV to observed FTV was greater than 1, the effect was considered to be synergistic. A ratio less than 1 suggested that the effect was additive.

Orthotopic tumor model

An orthotopic mouse PDAC model was generated in the pancreas of athymic mice, as previously described,[43] using the BxPC-3-Red-Fluc cells (1×10^6) suspended in 80 μL serum-free medium on day 0 with a 1-mL disposable syringe and a 26G needle. Tumor volume was evaluated using bioluminescence, which is highly specific and sensitive for tumor detection. Briefly, mice were anesthetized with isoflurane and intraperitoneally injected with 150 mg/kg of D-luciferin (Promega, Madison, WI, USA) as the substrate. For tumor detection, mice were placed in the right lateral decubitus position. Images were acquired 20 min after administration of luciferin. The signal intensity was evaluated as the sum of all detected photon counts within the region of interest after subtraction of background luminescence. In preliminary experiments, orthotopic tumors were observed to have a tumor diameter of approximately 4 mm on day 14, so the timing was chosen for treatment initiation. On day 14, each tumor volume was evaluated based on the bioluminescence, and mice were randomly assigned to mock and G47Δ treatment groups. After randomization, mice were anesthetized, and the abdominal wall was incised 1 cm to expose the pancreatic tumor. G47Δ (1×10^7 pfu) or mock was injected with a 100-μL Hamilton syringe and a 30G needle at a depth of 3 mm. The abdominal wall was closed with a 5-0 nylon surgical suture. Photons were counted every 3–4 days until day 49. The survival rate was evaluated until day 110.

In vitro cytotoxicity studies

In vitro cytotoxicity studies were performed as described previously.[44] Cytotoxicity studies in #146 cells were performed using DMEM with 10% heat-inactivated FBS. The number of surviving cells was counted every day with the Coulter Counter (Beckman Coulter, Brea, CA, USA) and expressed as percentage of the number of mock-infected control cells.

X-gal staining

Vero, #146, and human PDAC cells (Panc-1, Capan-1, Capan-2, and BxPC-3) were seeded in six-well plates (3×10^5 cells/well) and infected with G47Δ at an MOI of 1 or 3 at 37°C for 1 h, and further cultured for 4 h. Next, the cells were fixed with 0.2% glutaraldehyde or 2% paraformaldehyde and incubated with X-gal substrate solution (PBS, 5-bromo-4-chloro-3-indolyl-β-d-galactoside, 5 mM potassium ferricyanide, 5 mM potassium ferrocyanide, and 2 mM magnesium chloride) at 37°C for 2 h.

Virus replication assay

Vero and human PDAC cells (Panc-1, Capan-1, Capan-2, and BxPC-3) were seeded in six-well plates (3×10^5 cells/well) and infected with G47Δ at an MOI of 0.01. After incubation at 37°C for 24 or 48 h, cells were collected, and virus yields were assessed using plaque assay with Vero cells.

G47Δ and FAKi combination therapy in a subcutaneous tumor model

C57BL/6NCrSlc mice bearing established subcutaneous #146 tumors were treated with intratumoral injections with G47Δ (2×10^6 pfu) or mock on days 4 and 7. FAKi (VS-4718, Selleck, Houston, TX, USA) was administered orally (50 mg/kg) every day starting on day 4. VS-4718 is a selective bispecific inhibitor with activity against FAK1/FAK and FAK2/PYK2 kinases. VS-4718 has been shown to suppress tumor progression and prolong survival of transgenic KPC mice and to render pancreatic cancers responsive to ICIs.[18]

Combination therapy in transgenic PKF mice

In preliminary experiments, all PKF mice were observed to have more than 80% of the pancreas occupied by tumor at 42 days of age, so the timing was chosen for treatment initiation. 42-day-old PKF mice were treated with a single intratumoral injection with G47Δ (1×10^7 pfu), intraperitoneal injections with anti-PD-L1 antibody (clone 10F.9G2, BioXCell, Lebanon, NH, USA, 200 μg/body), and anti-CTLA4 antibody (clone 9H10, BioXCell, 250 μg/body) every 4–5 days starting on day 42. For G47Δ treatment, mice were anesthetized, and the abdominal wall was incised 1.5 cm to expose the pancreatic tumor. G47Δ was injected with a 100-μL Hamilton syringe and a 30G needle at a depth of 5 mm. The abdominal wall was closed with a 5-0 nylon surgical suture.

For the combination therapy of FAKi and ICIs, 42-day-old PKF mice started daily treatment of oral administration with FAKi (50 mg/kg) and received intraperitoneal injections with anti-PD-L1 (200 μg/body) and anti-CTLA4 (250 μg/body) antibodies every 4–5 days since day 42. For the triple combination therapy, PKF mice were treated with FAKi, anti-PD-L1, and anti-CTLA4 in the same manner as above, and a single intratumoral injection with G47Δ (1×10^7 pfu) on day 52. The rat IgG2b antibody (clone LTF-2, BioXCell) and Syrian Hamster IgG antibody (polyclonal, BioXCell) were used as isotype controls.

Flow cytometric analysis

C57BL/6NCrSlc mice bearing established subcutaneous #146 tumors were treated with intratumoral injections with G47Δ (2×10^6 pfu) or mock on days 4 and 7, and oral administrations with FAKi (50 mg/kg) daily from day 4. Tumors were excised on day 9, and mouse Tumor Dissociation Kit (Miltenyi Biotec, Bergisch Gladbach, Germany), gentleMACS Dissociator (Miltenyi Biotec), and gentleMACS C Tubes (Miltenyi Biotec) were used to prepare single cells according to the manufacturer's protocol. Red blood cells were removed by using the RBC lysis buffer (Thermo Fisher Scientific, Waltham, MA, USA). Single cells including TILs were stained with several antibodies (Table S1) and analyzed using the gating strategy (Figure S3). Cell subsets were defined as follows: $CD8^+$ lymphocytes ($CD45^+CD14^-CD19^-CD8^+$); $CD4^+$ lymphocytes ($CD45^+CD14^-CD19^-CD4^+$); NK cells ($CD45^+CD49b^+CD3^-$); Treg ($CD45^+CD14^-CD19^-CD4^+Foxp3^+$); $CD45^+PD\text{-}L1^+$ cells ($CD45^+PD\text{-}L1^+$); PD-$L1^+$ tumor cells ($CD45^-PD\text{-}L1^+$); TAM1 cells ($CD45^+CD3^-F4/80^+CD11b^+CD206^-CD86^+$), TAM2 cells ($CD45^+CD3^-F4/80^+CD11b^+CD206^+CD86^-$); M-MDSC ($CD45^+CD11b^+Ly6G^-Ly6C^{high}$); G-MDSC ($CD45^+CD11b^+Ly6G^+Ly6C^{low}$); $CD8^+CD69^+$ lymphocytes ($CD45^+CD3^+CD8^+CD69^+CD8^+$ $CD25^+$ lymphocytes ($CD45^+CD3^+CD8^+CD25^+$); $CD4^+CD69^+$ lymphocytes ($CD45^+CD3^+CD4^+CD69^+$); $CD4^+CD25^+$ lymphocytes ($CD45^+CD3^+CD4^+CD25^+$). The True-Nuclear Transcription Factor Buffer Set (BioLegend, San Diego, CA, USA) was used for intra-nuclear staining according to the manufacturer's protocol. The analysis was performed on the CytoFLEX flow cytometer (Beckman Coulter, Brea, CA, USA).

ELISpot assay

#146 cells (1×10^6) were implanted subcutaneously into the left flanks of C57BL/6NCrSlc mice. When tumors were established, mice received intratumoral injections with G47Δ (2×10^6 pfu) or mock on days 4 and 7 and oral administrations with FAKi (50 mg/kg) daily from day 4. Mice were sacrificed on day 9, and a single-cell suspension of splenocytes was prepared. After the splenocytes were stimulated by #146 cells, IFN-γ secretion from tumor-reactive splenocytes was evaluated using IFN-γ ELISpot PLUS (Mabtech, Nacka Strand, Sweden). Assays were conducted following the manufacturer's protocol. Spots were counted and analyzed using the ImmunoSpot Analyzer and ImmunoSpot software (CTL, Cleveland, OH, USA).

Histological analysis

Tumors were excised from subcutaneous #146 tumors of C57BL/6NCrSlc mice or pancreatic tumors of PKF mice and fixed in 10% formaldehyde neutral buffer solution (Sigma-Aldrich, St. Louis, MO, USA) for 72 h, and embedded in paraffin. Sections were rehydrated through graded alcohol, and Target Retrieval Solution S1700 (Agilent Technologies, Santa Clara, CA, USA) was used for heat-mediated antigen retrieval. A subcutaneous Neuro2a (neuroblastoma) tumor generated in syngeneic A/J mouse was used as a stroma-poor histology control. The sections were immunostained with anti-mouse CD161, CD86, CD206, CD8α, CD4, alpha smooth muscle actin (αSMA) antibody (Cell Signaling Technology, Danvers, MA, USA), or anti-HSV-1 antibody (Abcam, Cambridge, United Kingdom), followed by developing using the 3-3′ diaminobenzidine (DAB) as chromogenic substrate. For the measurement of $CD8^+$ cells, a blinded observer counted the number of positive cells in five fields (0.5 mm^2/field) per section.

Cytokine analysis

C57BL/6NCrSlc male mice with established subcutaneous #146 tumors were treated with intratumoral injections with G47Δ (2×10^6 pfu) on days 4 and 7 and daily oral administration with FAKi. Serum was collected from mice on days 4, 7, and 14 and was used for cytokine analysis. The levels of IFN-γ, IL-2, IL-4, IL-5, IL-6, IL-10, IL-12, TNF-α, and GM-CSF were evaluated using the Bio-Plex Multiplex Assay and Bio-Plex 200 system (Bio-Rad, Hercules, CA, USA) according to the manufacturer's protocol.

Detection of G47Δ by quantitative polymerase chain reaction

Subcutaneous #146 tumors in C57BL/6NCrSlc male mice were injected with G47Δ (2×10^6 pfu) on days 4 and 7. Tumors were excised on day 9, and DNA was extracted using the QIAamp Fast DNA Tissue Kit (QIAGEN, Venlo, the Netherlands). One HSV-specific primer pair, amplifying the glycoprotein B (gB) gene, was used. The forward primer sequence was 5′-GGCGCGGTCCTCAAAGAT-3′ and reverse primer sequence was 5′-AGAACATCGCCCCGTACAAG-3′. PCR was performed using the 7500 Fast Real-time PCR System (Thermo Fisher Scientific). HSV genome copy number below 1.0×10^5/ng DNA was not detectable. Approximately 36 copies of G47Δ detected by qPCR equal 1 pfu.

In vivo replication assay

Subcutaneous K399 tumors in athymic (BALB/c *nu/nu*) mice were injected with G47Δ (2×10^6 pfu) or mock 7 days after tumor

implantation. Tumors were harvested on days 0, 1, 2, 3, and 7 for G47Δ (n = 3–4) and on day 0 for mock (n = 3). DNA was extracted and qPCR for G47Δ was performed as described above.

Replication and cytotoxicity evaluation of G47Δ in the normal pancreas

G47Δ (1×10^7 pfu) or mock in a volume of 20 μL was injected into the pancreas of A/J mice using a 100-μL Hamilton syringe and a 30G needle. The pancreases injected with G47Δ were removed on days 0, 3, and 7 (n = 3 per day) and those with mock on day 0 (n = 3), and the amount of G47Δ DNA was measured by qPCR as described above. In a separate set of experiments, the pancreases of A/J mice were injected with G47Δ or mock, removed on days 0, 3, and 7 (n = 3 per day for both groups), and subjected to pathological evaluation by H&E staining and immunohistochemistry for HSV-1.

Statistical analysis

Two-tailed Student's *t* test was used for all comparisons, except for Kaplan-Meier analysis, for which a log rank test was used. In all cases, $p < 0.05$ was considered to be statistically significant. All statistical analyses were performed using the JMP Pro 14 software (SAS, Cary, NC, USA).

DATA AVAILABILITY

The datasets generated and/or analyzed during the current study are available from the corresponding author upon reasonable request.

SUPPLEMENTAL INFORMATION

Supplemental information can be found online at https://doi.org/10.1016/j.omto.2022.12.001.

ACKNOWLEDGMENTS

We thank Dr. Yasushi Ino for his advice in planning experiments and Kyoko Saiga, Eri Ozaki, and Rumi Takashima for their technical assistance. This research was supported in part by grants to T.T. from Practical Research for Innovative Cancer Control (Grant Number JP18ck0106416) and Translational Research Program (Grant Number JP17lm0203004), Japan Agency for Medical Research and Development (AMED).

AUTHOR CONTRIBUTIONS

T.Y. and T.T. were involved in the conception, design, and performance of experiments, statistical analyses, interpretation of results, and writing the manuscript. M.I., M.T., H.I., and M.S. assisted in designing and performing the experiments. R.T. and K.K. were involved in the conception and design of experiments. All the authors were involved in reviewing and editing the manuscript.

DECLARATION OF INTERESTS

Tomoki Todo owns the patent right for G47Δ in Japan.

REFERENCES

1. Rahib, L., Smith, B.D., Aizenberg, R., Rosenzweig, A.B., Fleshman, J.M., and Matrisian, L.M. (2014). Projecting cancer incidence and deaths to 2030: the unexpected burden of thyroid, liver, and pancreas cancers in the United States. Cancer Res. *74*, 2913–2921.
2. Von Hoff, D.D., Ervin, T., Arena, F.P., Chiorean, E.G., Infante, J., Moore, M., Seay, T., Tjulandin, S.A., Ma, W.W., Saleh, M.N., et al. (2013). Increased survival in pancreatic cancer with nab-paclitaxel plus gemcitabine. N. Engl. J. Med. *369*, 1691–1703.
3. Todo, T., Martuza, R.L., Rabkin, S.D., and Johnson, P.A. (2001). Oncolytic herpes simplex virus vector with enhanced MHC class I presentation and tumor cell killing. Proc. Natl. Acad. Sci. USA *98*, 6396–6401.
4. Cheema, T.A., Wakimoto, H., Fecci, P.E., Ning, J., Kuroda, T., Jeyaretna, D.S., Martuza, R.L., and Rabkin, S.D. (2013). Multifaceted oncolytic virus therapy for glioblastoma in an immunocompetent cancer stem cell model. Proc. Natl. Acad. Sci. USA *110*, 12006–12011.
5. Fukuhara, H., Ino, Y., and Todo, T. (2016). Oncolytic virus therapy: a new era of cancer treatment at dawn. Cancer Sci. *107*, 1373–1379.
6. Sugawara, K., Iwai, M., Yajima, S., Tanaka, M., Yanagihara, K., Seto, Y., and Todo, T. (2020). Efficacy of a third-generation oncolytic herpes virus G47Delta in advanced stage models of human gastric cancer. Mol. Ther. Oncolytics *17*, 205–215.
7. Yamada, T., Tateishi, R., Iwai, M., Koike, K., and Todo, T. (2020). Neoadjuvant use of oncolytic herpes virus G47Δ enhances the antitumor efficacy of radiofrequency ablation. Mol. Ther. Oncolytics *18*, 535–545.
8. Uchihashi, T., Nakahara, H., Fukuhara, H., Iwai, M., Ito, H., Sugauchi, A., Tanaka, M., Kogo, M., and Todo, T. (2021). Oncolytic herpes virus G47Δ injected into tongue cancer swiftly traffics in lymphatics and suppresses metastasis. Mol. Ther. Oncolytics *22*, 388–398.
9. Sugawara, K., Iwai, M., Ito, H., Tanaka, M., Seto, Y., and Todo, T. (2021). Oncolytic herpes virus G47Δ works synergistically with CTLA-4 inhibition through dynamic intratumoral immune modulation. Mol. Ther. Oncolytics *22*, 129–142.
10. Yajima, S., Sugawara, K., Iwai, M., Tanaka, M., Seto, Y., and Todo, T. (2021). Efficacy and safety of a third-generation oncolytic herpes virus G47Δ in models of human esophageal carcinoma. Mol. Ther. Oncolytics *23*, 402–411.
11. Todo, T., Ino, Y., Ohtsu, H., Shibahara, J., and Tanaka, M. (2022). A phase I/II study of triple-mutated oncolytic herpes virus G47Δ in patients with progressive glioblastoma. Nat. Commun. *13*, 4119.
12. Todo, T., Ito, H., Ino, Y., Ohtsu, H., Ota, Y., Shibahara, J., and Tanaka, M. (2022). Intratumoral oncolytic herpes virus G47Δ for residual or recurrent glioblastoma: a phase 2 trial. Nat. Med. *28*, 1630–1639.
13. Andtbacka, R.H.I., Kaufman, H.L., Collichio, F., Amatruda, T., Senzer, N., Chesney, J., Delman, K.A., Spitler, L.E., Puzanov, I., Agarwala, S.S., et al. (2015). Talimogene laherparepvec improves durable response rate in patients with advanced melanoma. J. Clin. Oncol. *33*, 2780–2788.
14. Desjardins, A., Gromeier, M., Herndon, J.E., 2nd, Beaubier, N., Bolognesi, D.P., Friedman, A.H., Friedman, H.S., McSherry, F., Muscat, A.M., Nair, S., et al. (2018). Recurrent glioblastoma treated with recombinant poliovirus. N. Engl. J. Med. *379*, 150–161.
15. Nakao, A., Kasuya, H., Sahin, T.T., Nomura, N., Kanzaki, A., Misawa, M., Shirota, T., Yamada, S., Fujii, T., Sugimoto, H., et al. (2011). A phase I dose-escalation clinical trial of intraoperative direct intratumoral injection of HF10 oncolytic virus in non-resectable patients with advanced pancreatic cancer. Cancer Gene Ther. *18*, 167–175.
16. Hecht, J.R., Bedford, R., Abbruzzese, J.L., Lahoti, S., Reid, T.R., Soetikno, R.M., Kirn, D.H., and Freeman, S.M. (2003). A phase I/II trial of intratumoral endoscopic ultrasound injection of ONYX-015 with intravenous gemcitabine in unresectable pancreatic carcinoma. Clin. Cancer Res. *9*, 555–561.
17. Mulvihill, S., Warren, R., Venook, A., Adler, A., Randlev, B., Heise, C., and Kirn, D. (2001). Safety and feasibility of injection with an E1B-55 kDa gene-deleted, replication-selective adenovirus (ONYX-015) into primary carcinomas of the pancreas: a phase I trial. Gene Ther. *8*, 308–315.
18. Jiang, H., Hegde, S., Knolhoff, B.L., Zhu, Y., Herndon, J.M., Meyer, M.A., Nywening, T.M., Hawkins, W.G., Shapiro, I.M., Weaver, D.T., et al. (2016). Targeting focal adhesion kinase renders pancreatic cancers responsive to checkpoint immunotherapy. Nat. Med. *22*, 851–860.
19. Serrels, A., Lund, T., Serrels, B., Byron, A., McPherson, R.C., von Kriegsheim, A., Gómez-Cuadrado, L., Canel, M., Muir, M., Ring, J.E., et al. (2015). Nuclear FAK

controls chemokine transcription, Tregs, and evasion of anti-tumor immunity. Cell *163*, 160–173.

20. Wilky, B.A. (2019). Immune checkpoint inhibitors: the linchpins of modern immunotherapy. Immunol. Rev. *290*, 6–23.
21. O'Reilly, E.M., Oh, D.Y., Dhani, N., Renouf, D.J., Lee, M.A., Sun, W., Fisher, G., Hezel, A., Chang, S.C., Vlahovic, G., et al. (2019). Durvalumab with or without tremelimumab for patients with metastatic pancreatic ductal adenocarcinoma: a phase 2 randomized clinical trial. JAMA Oncol. *5*, 1431–1438.
22. Royal, R.E., Levy, C., Turner, K., Mathur, A., Hughes, M., Kammula, U.S., Sherry, R.M., Topalian, S.L., Yang, J.C., Lowy, I., and Rosenberg, S.A. (2010). Phase 2 trial of single agent Ipilimumab (anti-CTLA-4) for locally advanced or metastatic pancreatic adenocarcinoma. J. Immunother. *33*, 828–833.
23. Renouf, D.J., Loree, J.M., Knox, J.J., Topham, J.T., Kavan, P., Jonker, D., Welch, S., Couture, F., Lemay, F., Tehfe, M., et al. (2022). The CCTG PA.7 phase II trial of gemcitabine and nab-paclitaxel with or without durvalumab and tremelimumab as initial therapy in metastatic pancreatic ductal adenocarcinoma. Nat. Commun. *13*, 5020.
24. Weiss, G.J., Blaydorn, L., Beck, J., Bornemann-Kolatzki, K., Urnovitz, H., Schütz, E., and Khemka, V. (2018). Phase Ib/II study of gemcitabine, nab-paclitaxel, and pembrolizumab in metastatic pancreatic adenocarcinoma. Invest. New Drugs *36*, 96–102.
25. Russell, S.J., and Barber, G.N. (2018). Oncolytic viruses as antigen-agnostic cancer vaccines. Cancer Cell *33*, 599–605.
26. Ijichi, H., Chytil, A., Gorska, A.E., Aakre, M.E., Fujitani, Y., Fujitani, S., Wright, C.V.E., and Moses, H.L. (2006). Aggressive pancreatic ductal adenocarcinoma in mice caused by pancreas-specific blockade of transforming growth factor-beta signaling in cooperation with active Kras expression. Genes Dev. *20*, 3147–3160.
27. Ijichi, H., Chytil, A., Gorska, A.E., Aakre, M.E., Bierie, B., Tada, M., Mohri, D., Miyabayashi, K., Asaoka, Y., Maeda, S., et al. (2011). Inhibiting Cxcr2 disrupts tumor-stromal interactions and improves survival in a mouse model of pancreatic ductal adenocarcinoma. J. Clin. Invest. *121*, 4106–4117.
28. Miyabayashi, K., Ijichi, H., Mohri, D., Tada, M., Yamamoto, K., Asaoka, Y., Ikenoue, T., Tateishi, K., Nakai, Y., Isayama, H., et al. (2013). Erlotinib prolongs survival in pancreatic cancer by blocking gemcitabine-induced MAPK signals. Cancer Res. *73*, 2221–2234.
29. Sano, M., Takahashi, R., Ijichi, H., Ishigaki, K., Yamada, T., Miyabayashi, K., Kimura, G., Mizuno, S., Kato, H., Fujiwara, H., et al. (2021). Blocking VCAM-1 inhibits pancreatic tumour progression and cancer-associated thrombosis/thromboembolism. Gut *70*, 1713–1723.
30. Hingorani, S.R., Wang, L., Multani, A.S., Combs, C., Deramaudt, T.B., Hruban, R.H., Rustgi, A.K., Chang, S., and Tuveson, D.A. (2005). Trp53R172H and KrasG12D cooperate to promote chromosomal instability and widely metastatic pancreatic ductal adenocarcinoma in mice. Cancer Cell *7*, 469–483.
31. Chard, L.S., Maniati, E., Wang, P., Zhang, Z., Gao, D., Wang, J., Cao, F., Ahmed, J., El Khouri, M., Hughes, J., et al. (2015). A vaccinia virus armed with interleukin-10 is a promising therapeutic agent for treatment of murine pancreatic cancer. Clin. Cancer Res. *21*, 405–416.
32. Rosenberg, A., and Mahalingam, D. (2018). Immunotherapy in pancreatic adenocarcinoma-overcoming barriers to response. J. Gastrointest. Oncol. *9*, 143–159.
33. Ko, A.H., LoConte, N., Tempero, M.A., Walker, E.J., Kate Kelley, R., Lewis, S., Chang, W.C., Kantoff, E., Vannier, M.W., Catenacci, D.V., et al. (2016). A phase I study of FOLFIRINOX plus IPI-926, a Hedgehog pathway inhibitor, for advanced pancreatic adenocarcinoma. Pancreas *45*, 370–375.
34. Hakim, N., Patel, R., Devoe, C., and Saif, M.W. (2019). Why HALO 301 failed and implications for treatment of pancreatic cancer. Pancreas (Fairfax) *3*, e1–e4.
35. Pang, X.J., Liu, X.J., Liu, Y., Liu, W.B., Li, Y.R., Yu, G.X., Tian, X.Y., Zhang, Y.B., Song, J., Jin, C.Y., and Zhang, S.Y. (2021). Drug discovery targeting focal adhesion kinase (FAK) as a promising cancer therapy. Molecules *26*, 4250.
36. Upadhrasta, S., and Zheng, L. (2019). Strategies in developing immunotherapy for pancreatic cancer: recognizing and correcting multiple immune "defects" in the tumor microenvironment. J. Clin. Med. *8*, 1472.
37. Pallmer, K., Barnstorf, I., Baumann, N.S., Borsa, M., Jonjic, S., and Oxenius, A. (2019). NK cells negatively regulate CD8 T cells via natural cytotoxicity receptor (NCR) 1 during LCMV infection. Plos Pathog. *15*, e1007725.
38. Iraolagoitia, X.L.R., Spallanzani, R.G., Torres, N.I., Araya, R.E., Ziblat, A., Domaica, C.I., Sierra, J.M., Nuñez, S.Y., Secchiari, F., Gajewski, T.F., et al. (2016). NK cells restrain spontaneous antitumor CD8+ T cell priming through PD-1/PD-L1 interactions with dendritic cells. J. Immunol. *197*, 953–961.
39. Sano, M., Ijichi, H., Takahashi, R., Miyabayashi, K., Fujiwara, H., Yamada, T., Kato, H., Nakatsuka, T., Tanaka, Y., Tateishi, K., et al. (2019). Blocking CXCLs-CXCR2 axis in tumor-stromal interactions contributes to survival in a mouse model of pancreatic ductal adenocarcinoma through reduced cell invasion/migration and a shift of immune-inflammatory microenvironment. Oncogenesis *8*, 8.
40. Havel, J.J., Chowell, D., and Chan, T.A. (2019). The evolving landscape of biomarkers for checkpoint inhibitor immunotherapy. Nat. Rev. Cancer *19*, 133–150.
41. Ichimaru, Y., Sano, M., Kajiwara, I., Tobe, T., Yoshioka, H., Hayashi, K., Ijichi, H., and Miyairi, S. (2019). Indirubin 3'-oxime inhibits migration, invasion, and metastasis InVivo in mice bearing spontaneously occurring pancreatic cancer via blocking the RAF/ERK, AKT, and SAPK/JNK pathways. Transl. Oncol. *12*, 1574–1582.
42. Yu, D.C., Chen, Y., Dilley, J., Li, Y., Embry, M., Zhang, H., Nguyen, N., Amin, P., Oh, J., and Henderson, D.R. (2001). Antitumor synergy of CV787, a prostate cancer-specific adenovirus, and paclitaxel and docetaxel. Cancer Res. *61*, 517–525.
43. Réjiba, S., Bigand, C., Parmentier, C., and Hajri, A. (2009). Gemcitabine-based chemogene therapy for pancreatic cancer using Ad-dCK::UMK GDEPT and TS/RR siRNA strategies. Neoplasia *11*, 637–650.
44. Todo, T., Rabkin, S.D., Sundaresan, P., Wu, A., Meehan, K.R., Herscowitz, H.B., and Martuza, R.L. (1999). Systemic antitumor immunity in experimental brain tumor therapy using a multimutated, replication-competent herpes simplex virus. Hum. Gene Ther. *10*, 2741–2755.